Astron. Astrophys. 338, 31–42 (1998)

ASTRONOMY AND ASTROPHYSICS

X-ray observations of the interacting system Arp 284

P. Papaderos⋆ **and K.J. Fricke**

Universitäts Sternwarte, Geismarlandstraße 11, D-37083 Göttingen, Germany

Received 27 February 1998 / Accepted 10 July 1998

Abstract. We discuss the X-ray properties of the interacting system Arp 284, consisting of the active nuclear starburst galaxy NGC 7714 and its post-starburst companion NGC 7715. A morphological signature of the interaction, thought to have started < 100 Myr ago, is an asymmetric stellar ring dominating the intensity profile of NGC 7714 in the inner disk (~ 2 exponential scale lengths). In agreement to previous *Einstein*-data our ROSAT PSPC exposure shows the X-ray emission of Arp 284 to be confined to NGC 7714. The bulk of the intrinsic X-ray luminosity in the ROSAT 0.1–2.4 keV band can be accounted for by thermal emission from hot ($\sim 5 \times 10^6$ K) gas and amounts to $\sim 2 - 4 \times 10^{41}$ erg s^{-1}. Follow-up observations with the ROSAT HRI revealed two distinct extended emitting regions contributing to the X-ray luminosity in NGC 7714. The more luminous of them ($L_{\rm X} \lesssim 2 \times 10^{41}$ erg s^{-1}) coincides with the central starburst nucleus and can be explained this way. The fainter one ($L_{\rm X} \sim 8 \times 10^{40}$ erg s^{-1}) is located $\sim 20''$ off-center and does not have any conspicuous optical counterpart. It is, likely, located at the borderline between the stellar ring and a massive ($> 10^9$ M$_\odot$) H I-bridge further to the east possibly intersecting NGC 7714. The H I and X-ray morphology and the extensive starburst nature of the nuclear energy source suggest different scenarios for the formation of the eastern emission spot. The possibilities of (i) collisional heating of the outlying gas by a starburst-driven nuclear wind and (ii) infall of H I-clouds from the bridge onto the disk of NGC 7714 are discussed.

Key words: galaxies: individual: Arp 284 = NGC 7714-15 – galaxies: interaction – galaxies: photometry – galaxies: starburst – X-rays: galaxies

1. Introduction

Observational work during the past two decades has established the paradigm of interaction-induced activity in galaxies (cf. Fricke & Kollatschny 1989; Sulentic 1990). Galaxy interactions were initially studied theoretically by simplified N-body simulations (Toomre & Toomre 1972) and investigated in more detail by N-body/SPH models (Barnes & Hernquist 1996 and references therein). Interactions are linked to a variety of physical processes such as nuclear starbursts, non-thermal nuclear activity, and morphological evolution into different classes of galaxies (Barnes & Hernquist 1992). Already, collisionless calculations can simulate the transformation of merged spirals into ellipticals (Schweizer 1982) and the formation of tidal dwarf galaxies (Duc & Mirabel 1994; Sanders & Mirabel 1996). Thereby, understanding galaxy interactions is a prerequisite for addressing issues like the morphological mix and the luminosity and number distribution of galaxies. Gravitational perturbations of the gas component through encounters between spirals can provoke large-scale internal gas instabilities, loss of angular momentum, and inflow of gas into the nuclear regions. Accumulation of gas at high densities (Solomon et al. 1992) is thought to be a necessary condition for the onset of vigorous nuclear starbursts (Sanders & Mirabel 1996 and references therein) or even the development of AGN activity. In the presence of dust, the radiative output of massive stellar clusters is absorbed and reradiated in the far-infrared, a process which is thought to operate in the class of FIR-luminous galaxies. At the same time, the collective output of energy and momentum from OB stars and supernovae explosions into the interstellar medium creates a hot ($\sim$ few 10^6 K) X–ray emitting gas phase. The thermal pressure exerted by this component on the ambient cold gas may terminate the gas-inflow and even disrupt the outlying H I-layer, thus giving rise to a fast ($\sim 10^3$ km sec^{-1}) galactic wind (Heckman et al. 1987;1996, Veilleux et al. 1994).

On the other hand, interactions between galaxies may effect a redistribution of a large fraction of the cold gaseous component on scales of hundreds of kpc. H I-plumes or bridges emanating from the nuclear regions or protruding from the plane do not seem to be uncommon among interacting/merging galaxies. Gaseous features on scales of 50 to 150 kpc and mass ranges between 1.5 and $\sim 6 \times 10^9$ M$_\odot$ were discovered in systems spanning a wide range across the merging sequence, such as Arp 144 (Higdon 1988), Arp 215 (Smith 1991), NGC 520 (Norman et al. 1996) and NGC 3256 (Hibbard & van Gorkom 1996). The fate of this material, in particular the question, whether it

Send offprint requests to: P. Papaderos

⋆ Visiting Astronomer, German-Spanish Astronomical Centre, Calar Alto, operated by the Max-Planck-Institute for Astronomy, Heidelberg, jointly with the Spanish National Commission for Astronomy

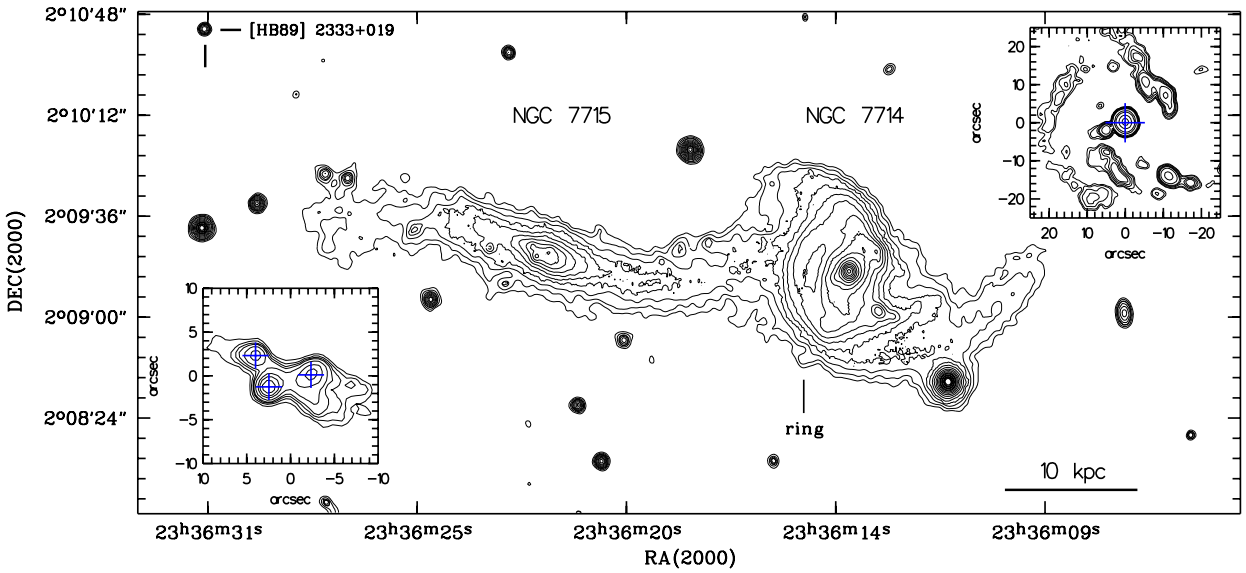

Fig. 1. Contour map of Arp 284 in the R band. Contours, corrected for galactic extinction (0.085 mag), are shown between levels 16.3 $\mathrm{mag\ arcsec^{-2}}$ to 24.3 $\mathrm{mag\ arcsec^{-2}}$ in steps of 0.5 mag. The nuclear regions of both galaxies are separated by 1.′96 (22.8 kpc). The marked stellar ring in NGC 7714 is best visible at $\sim 21.25\ \mathrm{mag\ arcsec^{-2}}$. The position of the background QSO [HB89] 2333+019 at z: 1.871 is indicated. Note the faint ($\mu_{\mathrm{R}} \gtrsim 23\ \mathrm{mag\ arcsec^{-2}}$) optical bridge connecting both systems. The insets to the lower-left and upper-right display the central 20″ × 20″and 50″×50″ regions of NGC 7715 and NGC 7714, respectively, after processing with the hb-method.

is going to be recaptured in the gravitational field of the merged system, is uncertain. It is, however, conceivable that after some time reinfall of tidally ejected matter onto a merger (Hibbard & Mihos 1995) could lead to shock formation, thereby provoking extranuclear activity or feeding a subsequent burst of star formation.

In this paper we focus our attention on the X-ray properties of the interacting system Arp 284 (Arp 1966). This system consists of the nuclear starburst galaxy NGC 7714 and its fainter inactive companion NGC 7715. Weedman et al. (1981) have first pointed out the extraordinary properties of NGC 7714 among starburst nuclei and inferred from *Einstein* observations an intrinsic X-ray luminosity of $0.6 \div 1 \times 10^{41}\ \mathrm{erg\ s^{-1}}$ in the 0.25–3.5 keV energy range. Other observational support for the presence of an ongoing burst of star formation in NGC 7714 is provided by the detection of WR spectral features and strong Hα emission on scales of $\sim 12''$ (González-Delgado et al. 1995, Smith et al. 1997, Telles & Terlevich 1997). Spectral synthesis models of Bernlöhr (1993) imply for NGC 7714 a burst age of ~ 20 Myr. The same author concluded that the less massive interaction counterpart NGC 7715 has undergone a burst of star formation roughly 70 Myr ago (Bernlöhr 1993), presumably at the time of the initial impact between both galaxies (Smith et al. 1992). Arp 284 displays features predicted to evolve shortly after the first closest passage between two gas-rich spirals (Smith et al. 1997, Hernquist 1992). A striking one is a large asymmetric ring located $\sim 20''$ eastwards of the nucleus of NGC 7714. Narrow-band imaging of NGC 7714 has not revealed a notable contribution of Hα emission to the light of this feature (González-Delgado et al. 1995, Smith et al. 1997). Also high angular resolution 21 cm VLA-maps of Arp 284 (Smith et al. 1997) show that the ring is comparatively devoid of H I-gas. Furthermore, Bushouse & Werner (1990) have reported that the stellar ring possesses NIR colours similar to those in the disk. All latter facts lend support to the idea that its formation process is related to a collisionally induced dynamical perturbation of the stellar disk (Lynds & Toomre 1976) rather than being the result of past star formation. This hypothesis is in accord with numerical simulations of off-center encounters between spiral galaxies demonstrating the formation of similar morphological features (Mihos & Hernquist 1996, Smith et al. 1992,1997). In the following we investigate the X-ray properties of Arp 284 using recent ROSAT data, together with relevant optical and radio observations. We shall adopt a distance of 40 Mpc (H_0=75 km $\mathrm{sec^{-1}\ Mpc^{-1}}$) to Arp 284 (Bernlöhr 1993).

2. Optical data

Arp 284 was observed with the 2.2m telescope at Calar Alto with a SITe-CCD detector attached to the CAFOS focal reducer giving an instrumental scale of $0.''53\,\mathrm{pixel^{-1}}$. The target was observed for 3 min in the Johnson R under non-photometric conditions with a seeing of $2.''1 \pm 0.''05$. The image was calibrated on the basis of aperture photometry by Bushouse & Werner (1990) and Bernlöhr (1993). The detection limit of point sources at a S/N of 2 was estimated to ~ 20.3 R mag. As shown in Fig. 1, the nuclear regions of the interacting galaxies NGC 7714 and NGC 7715 are separated by $\sim 1.'96$, corresponding to a linear distance of 22.8 kpc. Both galaxies are apparently connected by a diffuse and faint ($\mu_{\mathrm{R}} \gtrsim 23\ \mathrm{mag\ arcsec^{-2}}$) stellar bridge protruding from NGC 7715 into the outer boundary of the stellar ring in NGC 7714. The point source indicated to the upper-left is the QSO [HB89] 2333+019 $(\alpha, \delta)_{2000}$: $23^{\mathrm{h}}36^{\mathrm{m}}30^{\mathrm{s}}.5$,+02°

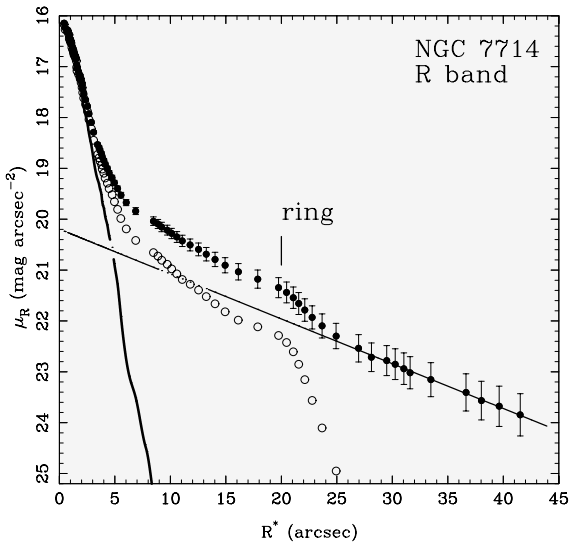

Fig. 2. Surface brightness profile of NGC 7714 in the R-band. The profile is not corrected for inclination. The luminosity distribution of the disk component (solid light line) is obtained by a linear fit to the outer part ($R^* > 25''$) of the profile, weighted by the photometric uncertainties. Open symbols display the residual intensity distribution in excess of the disk component. The intensity decrease by roughly 0.4 mag in the surface brightness profile of NGC 7714 at $R^* \approx 20''$ reflects the transition from the (bar+ring) component to the disk-dominated regime. The angular distance below which the disk dominates the light is $25''$ corresponding to ~ 2 disk exponential scale lengths (2.39±0.6 kpc). The luminosity distribution of the compact starburst nucleus is shown by the thick solid line. Its apparent luminosity integrated for $\mu_R \leq 25$ mag arcsec^{-2} is determined to 13.5 mag, equivalent to ~ 50% of the luminosity of NGC 7714 in excess of the disk.

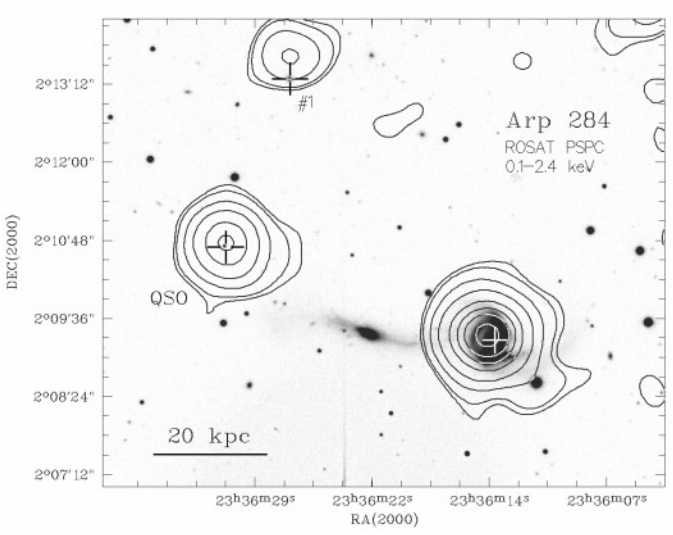

Fig. 3. ROSAT PSPC contours of the 0.1–2.4 keV emission of Arp 284 superimposed on an optical image. The X–ray image was convolved with a Gaussian with fwhm $35''$, equivalent to the average resolution of the PSPC camera in the 0.1–2.4 keV energy band. The positions of the QSO [HB89] 2223+019 and of the starburst nucleus of NGC 7714 are indicated by crosses. The X–ray source designated #1 is presumably associated with a faint background galaxy (cross). Contours correspond to intensities of 0.75, 1, 2, 4, 8, 12, 16 and 22 counts ksec^{-1} arcmin^{-2} *above* the background (0.87 ± 0.36 counts ksec^{-1} arcmin^{-2}).

$10'\,42''$ (Hewitt & Burbidge 1989). The apparent luminosity of this background source ($z = 1.871$) was determined to $m_{\rm R} = 18.6 \pm 0.1$ mag.

For the sake of revealing faint compact structures we processed the central region of NGC 7715 and NGC 7714 with a hierarchical binning algorithm (hereafter hb-method) designed for extracting weak features of angular size smaller than a user-defined angular threshold. Results obtained by the hb-method for the central regions of NGC 7714 and NGC 7715 are displayed in the insets in Fig. 1. The dominant features in NGC 7714 within a region of $\lesssim 12''$ in diameter are the compact starburst nucleus and an adjacent fainter knot. As shown in Fig. 2 the intensity distribution of NGC 7714 can be approximated reasonably well by an exponential fitting law for $\mu_R \gtrsim 22.5$ mag arcsec^{-2} . The marked intensity depression by ~ 0.4 mag in the SBP of NGC 7714 at a photometric radius $R^* \sim 20''$ reflects the sharp transition from the (bar+ring)–dominated regime of NGC 7714 to its fainter disk population.

3. X-ray data

We observed Arp 284 in the 0.1–2.4 keV energy band with both, the Position Sensitive Proportional Counter (PSPC) and the High Resolution Imager (HRI) on board ROSAT (Trümper 1983, Pfeffermann et al. 1987). The analysis of the X–ray data was carried out with the EXSAS package (Zimmermann et al. 1994) implemented in the MIDAS.

3.1. PSPC observations

Arp 284 was observed with the PSPC twice (PSPC_1: 1.33 and PSPC_2: 12.68 ksec). In both observations, intervals with a count rate exceeding by 3σ the mean value were screened out. We also checked that the aspect solution provided by the Standard Analysis Software System (SASS, Voges et al. 1992) does not contain residual aspect errors greater than $2''$. After the latter corrections we obtained effective exposures of 1.3 ksec and 12.1 ksec for PSPC_1 and PSPC_2, respectively. Our ROSAT PSPC exposure (Fig. 3) confirm the outcome of a preceding analysis of *Einstein*-IPC data (Fabbiano et al. 1992), namely that the entire soft X-ray emission in Arp 284 is confined to NGC 7714. The source to the left was registered at a PSPC count rate of $(8.3 \pm 2.8) \times 10^{-3}$ counts sec^{-1} . Follow-up observations with the ROSAT HRI (Sect. 3.2), show it to coincide with the background QSO [HB89] 2333+019. Its PSPC-spectrum, extracted within a circular aperture of radius $100''$, appears highly absorbed (HR_1=+0.89± 0.03)[1] and intrinsically rather hard (HR_2=+0.39±0.17). The X-ray source designated

[1] Hardness ratios are obtained from the *net* counts of a source as $HR_1 = (Hard - Soft)/(Hard + Soft)$ and $HR_2 = (H2 - H1)/(H1 + H2)$ registered in the standard ROSAT PSPC bands *Soft* (0.1-0.4 keV), *Hard* (0.5-2.0 keV), *H1* (0.5-0.9 keV) and *H2* (0.9-2.0 keV).

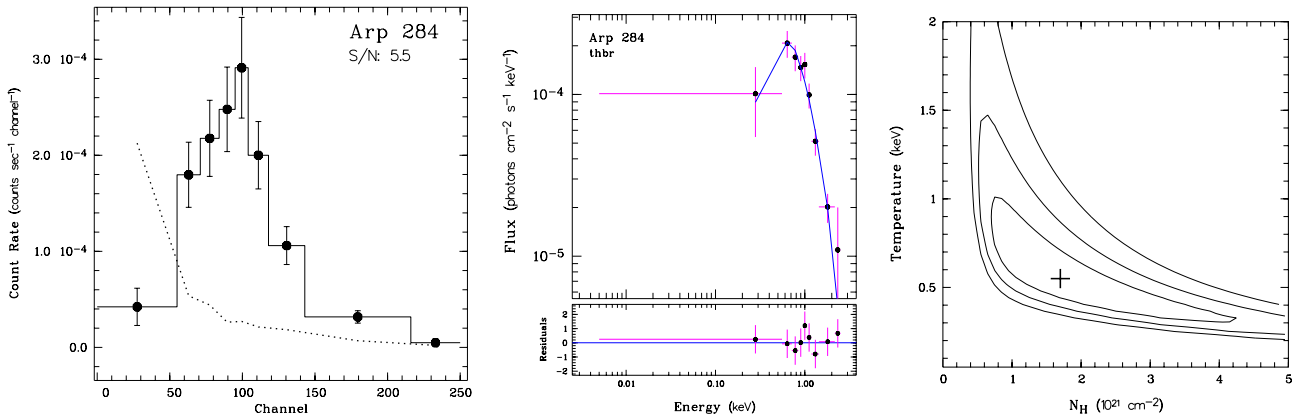

Fig. 4. *(left)* ROSAT PSPC spectrum of NGC 7714. The dotted curve displays the channel pulse height distribution of the X-ray background. The hardness ratios of the spectrum, $HR_1 = 0.87 \pm 0.03$ and $HR_2 = 0.20 \pm 0.13$ suggest a highly absorbed source with an intermediately hard intrinsic photon distribution. *(middle)* Unconstrained thermal bremstrahlung *(thbr)* fit to the soft X-ray spectrum of NGC 7714. Residuals to the observed flux distribution are displayed at the bottom panel. *(right)* χ^2 map for a *thbr* model as function of the absorbing gas column density (N_H) and the mean plasma temperature (kT). The contours correspond to confidence levels of 68.3, 95.4 and 99.7%. The deduced fit solution (Table 1) is indicated by the cross.

Table 1. Model fits to the ROSAT PSPC spectrum

Model	N_H^a 10^{21} cm^{-2}	kT keV	Γ	Flux^b (0.1-2.4 keV) 10^{-13} erg s^{-1} cm^{-2}	Flux^c (0.1-2.4 keV) 10^{-12} erg s^{-1} cm^{-2}	L_X (0.1-2.4 keV) 10^{41} erg s^{-1}	$\chi^2/d.o.f^d$
thbr	$1.7^{+2.56}_{-0.99}$	$0.55^{+0.46}_{-0.25}$	—	$2.39^{+3.31}_{-0.84}$	$1.04^{+1.43}_{-0.36}$	$2.0^{+2.8}_{-0.70}$	0.51
thbr(F1)	2.2	$0.47^{+0.08}_{-0.03}$	—	$2.28^{+0.04}_{-0.03}$	$1.41^{+0.03}_{-0.02}$	$2.7^{+0.06}_{-0.04}$	0.45
thbr(F2)	2.55	$0.43^{+0.08}_{-0.03}$	—	$2.22^{+0.04}_{-0.03}$	$1.74^{+0.03}_{-0.02}$	$3.3^{+0.06}_{-0.04}$	0.48
powl	$0.9^{+0.6}_{-0.2}$	—	2.3	$2.80^{+0.32}_{-0.49}$	$0.83^{+0.10}_{-0.15}$	$1.6^{+0.2}_{-0.3}$	1.19
bbdy	$0.5^{+1.97}_{-0.34}$	$0.24^{+0.04}_{-0.05}$	—	$2.30^{+0.9}_{-1.5}$	$0.31^{+0.12}_{-0.20}$	$0.6^{+0.23}_{-0.39}$	0.52

[a] Absorbing gas column density from a foreground screen model combining the Galactic H I column density $n_H^G = 0.493 \times 10^{21}$ cm^{-2} to the direction of Arp 284 (Dickey & Lockman 1990) with the intrinsic column density n_H^i of the target.
thbr: Unconstrained fit. N_H has been fitted from the X-ray data.
F1,F2: Constrained fits. The average intrinsic absorption n_H^i is estimated from the H I VLA-maps (Smith et al. 1997) on the basis of two different assumptions. F1: Each of the X-ray emitting regions within NGC 7714 (cf. Sect. 3.2) experiences a different amount of intrinsic absorption, and F2: Either emitting source resides midway in the H I-disk of NGC 7714 and experiences the same amount of intrinsic absorption.
[b] *absorbed* flux.
[c] *intrinsic* flux.
[d] χ^2 per degree of freedom (*d.o.f.*)

#1 is most probably associated to a faint ($m_R = 17.2$) background galaxy at $(\alpha, \delta)_{2000}$: $23^h36^m26^s.6$, $02°13' 17''$.

NGC 7714 was detected at a PSPC count rate of $(2.13 \pm 0.45) \times 10^{-2}$ counts sec^{-1} , yielding 286±60 source counts for the coadded PSPC_1 + PSPC_2 exposures. Its photon spectrum (Fig. 4, left) was extracted from a circular aperture of radius $135''$ and binned to a $S/N \sim 5.5$. The count rates registered in the *standard* ROSAT PSPC energy bands *Soft*, *Hard*, *H1* and *H2* are $(0.13 \pm 0.02) \times 10^{-2}$, $(1.9 \pm 0.34) \times 10^{-2}$, $(0.74 \pm 0.14) \times 10^{-2}$ and $(1.11 \pm 0.21) \times 10^{-2}$ counts sec^{-1}, respectively. The corresponding hardness ratios, $HR_1 = 0.87 \pm 0.03$ and $HR_2 = 0.20 \pm 0.13$, suggest a highly absorbed, intermediately hard spectrum. The hardness of the observed photon distribution complicates a precise assessment of the intrinsic absorbing column density n_H^i within NGC 7714. This is because n_H^i when deduced from unconstrained spectral fits is sensitively related to the spectral distribution below ~ 0.7 keV. Given that in the latter energy range the X-ray background becomes comparable or larger than the source flux the model-dependent n_H^i can significantly vary depending on the background determination. In order to study this effect we performed a number of tests by selecting background photons from different circular annuli and binning the resulting photon spectrum to a varying S/N. By applying a thermal bremsstrahlung model we have obtained two typical sets of solutions for n_H^i and the plasma temperature kT differing only marginally in terms of χ^2. The first one implies n_H^i; $kT \sim 1.2 \times 10^{21}$ cm^{-2};$\lesssim 0.55$ keV ($\chi^2/d.o.f \sim 0.5$; Table 1) and the second one $n_H^i, kT \sim 2.5 \times 10^{21}$ cm^{-2}; 0.4 keV with ($\chi^2/d.o.f \sim 0.7$). The corresponding lower and upper values for the intrinsic 0.1–2.4 keV luminosity of NGC 7714 are amounting to 2 and 4.4×10^{41} erg s^{-1}, respectively. Next we shall investigate constrained fits, in which the intrinsic absorbing column density is estimated from HI-maps. From VLA-studies, Smith et al. (1997) have determined within a

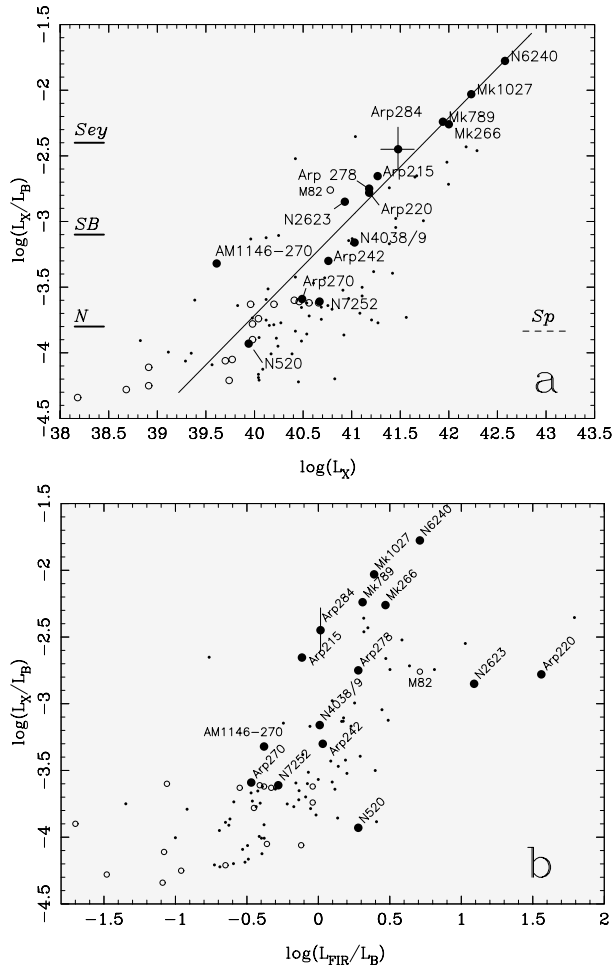

Fig. 5a and b. Comparison of Arp 284 with a sample of interacting/merging galaxies (filled circles) compiled from Read & Ponman (1998), Kollatschny et al. (1996), Wang et al. (1997), Fricke & Papaderos (1996) and Papaderos & Fricke (1998) in the $\log(L_X)$ vs. $\log(L_X/L_B)$ (top) and $\log(L_{FIR}/L_B)$ vs. $\log(L_X/L_B)$ planes (bottom). The bars indicate the positional shift of Arp 284 in the diagrams when a range of the intrinsic X-ray luminosity between 2 and 4×10^{41} erg s^{-1} is adopted. A linear fit (solid line, upper diagram) to the colliding galaxies implies a relation $\log(L_X/L_B) \propto$ 3/4 $\log(L_X)$. The mean ratio $\log(L_X/L_B) = -3.83$ for the sample of undisturbed spirals (open symbols; Read et al. 1997) is indicated by the dashed horizontal line (Sp). The mean $\log(L_X/L_B)$ ratios for quiescent (N), starburst (SB), and Seyfert (Sey) galaxies investigated with *Einstein* (David et al. 1992; small dots) are shown by the thick lines.

region of $11'' \times 8''$ centered at the starburst nucleus of NGC 7714 a mean H I column density of $\sim 4.1 \times 10^{21}$ cm^{-2}. As we shall show in Sect. 3.2, the HRI-X-ray emission of NGC 7714 is contributed by two distinct emitting sources. The most luminous one contributing $\sim 2/3$ of the received photons coincides with the nuclear region while the second one is off-centered and coincides with a region with a lower H I-column density. We may assume that the nuclear source resides midway in the H I-disk of NGC 7714, thus experiencing an intrinsic absorption $n_H^i \sim 2.05 \times 10^{21}$ cm^{-2} and the extranuclear source $n_H^i \sim 1 \times 10^{21}$ cm^{-2}. Weighting the latter values by the number of received photons we obtain an average intrinsic column density $n_H^i \sim 1.7 \times 10^{21}$ cm^{-2}. A *thbr* fit with $N_H = n_H^i + n_H^G$, where $n_G^H = 0.49 \times 10^{21}$ cm^{-2} is the Galactic column density, results in an intrinsic luminosity of 2.7×10^{41} erg s^{-1} (Table 1; F1). This luminosity estimate will increase to $L_X \sim 3.3 \times 10^{41}$ erg s^{-1}, if one assumes that either emitting region in NGC 7714 reside midway in the galactic plane, thus both experience an intrinsic absorption $n_H^i \sim 2 \times 10^{21}$ cm^{-2} (Table 1; F2).

In view of the starburst nature of NGC 7714 we consider a thermal bremsstrahlung (*thbr*) model to provide a reasonable approximation to its intrinsic soft X-ray spectrum.

A Raymond-Smith (1977) model was applied to the data assuming various elemental abundances, giving, however, unacceptable results in terms of χ^2 and implying in all cases an excessive absorbing gas column density ($> 8 \times 10^{21}$ cm^{-2}). A black-body fit to the spectrum leads to a χ^2 value comparable to the one obtained by applying a *thbr* model. However, it implies no intrinsic absorption within NGC 7714 in disagreement to the radio measurements. A power-law *(powl)* model, with a fixed photon index $\Gamma = 2.3$, which is the typical value found for extragalactic objects with ROSAT (Hasinger et al. 1991) yields an $N_H \sim 0.9 \times 10^{21}$ cm^{-2}, most probably incompatible with the average gas surface density inferred by Smith et al. (1997). Moreover, given that optical spectroscopy does not indicate the presence of an additional AGN source in NGC 7714 we will discard the *powl* model.

Adopting the mean value of $\sim 3 \times 10^{41}$ erg s^{-1} for the X-ray luminosity and estimating the B and FIR luminosities from the RC3– and the IRAS-PSC-catalogue following Tully (1988) and Devereux & Eales (1989), respectively, we obtain the ratios $\log(L_X/L_B) = -2.45$ and $\log(L_X/L_{FIR}) = -2.46$ for Arp 284.

In Fig. 5 we compare Arp 284 in the $\log(L_X)$ vs. $\log(L_X/L_B)$ and $\log(L_{FIR}/L_B)$ vs. $\log(L_X/L_B)$ diagrams with the location of the other interacting/merging galaxies: Arp 270, Arp 242, NGC 4038/9, NGC 520, Arp 220, NGC 2623, NGC 7252, AM 1146-270 (Read & Ponman 1998), Mkn 789, Mkn 1027 (Kollatschny et al. 1996), Mkn 266 (Wang et al. 1997), NGC 6240 (Fricke & Papaderos 1996) and Arp 278, Arp 215 (Papaderos & Fricke 1998). Open circles show the sample of isolated spirals discussed in Read et al. (1997). Small dots show the sample of *Einstein*-detected normal, starburst and Seyfert galaxies studied by David et al. (1992), adapted to $H_0 = 75$ km sec^{-1} Mpc^{-1}. Since the X-ray luminosities used by the latter authors refer to the 0.5–4.5 keV energy range they were shifted by $\delta \log(L_X) = -0.045$ to adapt them to the ROSAT energy band. For this purpose we assumed a *thbr* spectrum with $kT = 5$ keV for their sample. Arp 284 falls into the upper range in both diagrams for colliding galaxies. Fig. 5a shows a narrow linear correlation between $\log(L_X/L_B)$ and $\log(L_X)$: $\log(L_X/L_B) \propto 0.75 \pm 0.15 \log(L_X)$. A similar but less pronounced trend is seen in Fig. 5b correlating $\log(L_X/L_B)$ with $\log(L_{FIR}/L_B)$. These trends are reminiscent of the correspondence between the flux ratios X/B with the flux ratio Hα/B of interacting galaxies (Wang et al. 1997) and support the view that the strong X-ray emission from colliding galaxies

is not due to a global process but is closely tied to the starburst activity induced in such systems.

3.2. HRI observations

Arp 284 was observed with the HRI-camera for 45.86 ksec from 26 through 29 December 1994. Each observation combines data recorded over several satellite orbital intervals (OBIs). We verified that none of the OBIs was mispointed by comparing images constructed for each individual observation of duration greater than 1 ksec. After correction for residual aspect errors and rejection of time intervals with enhanced background emission we obtained a net exposure time of 45.6 ksec. The astronomical position of the targets as provided by the SASS was checked by registering the position of the QSO [HB89] 2333+019 at the optical image (Fig. 1). We deduced a residual aspect error of $\sim 8''$, compatible to the typical residual boresight error of $6''$ ascribed to SASS. The QSO was detected at a net source rate of $(1.9 \pm 0.7) \times 10^{-3}$ counts sec^{-1} , thereby making unfeasible to monitor residual wobbling errors in intervals shorter than the wobbling period (400 sec; cf. Bischoff et al. 1996) and improve on the short term aspect solution provided by the SASS. For the same reason other rectification methods, such as the one proposed by Morse (1994) and Güdel & Kürster (1996) were not applied to the data.

Fig. 6 displays the X-ray emission of NGC 7714 as obtained from ROSAT HRI observations. The gray map shows a number of weak optical features in NGC 7714's central region, revealed by the hb-technique. The optical extent of NGC 7714 at an extinction-corrected surface brightness of $\mu_{\rm R} = 23$ mag arcsec^{-2} is shown by the thin contour. Optical features designated **I** and **II**, both located westwards of the nucleus, were found to possess Hα emission (Bernlöhr 1993, González-Delgado et al. 1995) implying an ongoing extranuclear star-formation activity. The starburst nucleus indicated by the cross appears very compact (diameter $\lesssim 7''$) with a fainter knot located $\sim 5\farcs7$ to the east. From this knot proceeds a faint arm connecting to region **I**. The overlayed thick lines are computed from the ROSAT HRI exposure, convolved with a Gaussian with fwhm $5''$, equivalent to the nominal on-flight resolution of the camera. Fig. 6 reveals two discrete X-ray emitting components within the optical size of NGC 7714. The most luminous one (N) coincides with the starburst nucleus of NGC 7714 while component E is offset with respect to the former by $\sim 20''$. In view of possible interpretations of the origin of the extranuclear X-ray emitting component E (Sect. 4.2) it is notable that its location does not coincide with any conspicuous compact optical feature but rather appears associated with the clumpy luminosity pattern defined by the asymmetric stellar ring. The number of *net* counts in regions E and N are 112$\pm$16 and 221$\pm$22 (cf. Table 2), corresponding to count rates of 2.48$\pm$0.36 counts ksec^{-1} and 4.85$\pm$0.46 counts ksec^{-1}, respectively. Due to the low count rate a variability check for each knot separately proves not feasible. A variability check for NGC 7714 as whole carried out on both PSPC- and HRI-data has not revealed any systematic flux variations.

Unfortunately, the assessment of the spectral properties of each of the X-ray emitting components is being hampered by their low angular separation. While deconvolution of the PSPC data in the $H2$ band using an energy-weighted model for the Point Response Function (PRF) has clearly demonstrated the E-W elongation of the source, the quality of the data does not permit to put firm constraints on the spatial variation of the PSPC hardness ratio (cf. Read et al. 1995).

The ROSAT HRI is known to possess some moderate energy resolution. Thus, we checked the HRI softness ratios (counts in channels 1-5 divided by counts in channels 6-11; Wilson et al. 1992) deduced to 1.1$\pm$0.2 and 1.6$\pm$0.5 for component N and E, respectively. Although they suggest a slightly softer spectrum for component E they still, given the uncertainties, do not discard the possibility that either source share similar spectral properties. Furthermore, $\sim$ 90% of the flux of both components was received in channels 3-9 possibly making this method not appropriate for our data.

Assuming that the spectral properties of either source can be approximated by the unconstrained *thbr* fit (Table 1) one obtains for the HRI *energy conversion factor* (ECF; ROSAT Technical Appendix) 6.24×10^{-2}. Thereby, the source count rates translate to intrinsic fluxes of $(3.97 \pm 0.6) \times 10^{-13}$ erg s^{-1} cm^{-2} and $(7.78 \pm 0.75) \times 10^{-13}$ erg s^{-1} cm^{-2} for regions E and N, respectively, corresponding to component luminosities of $(7.6 \pm 1.1) \times 10^{40}$ erg s^{-1} and $(1.49 \pm 0.15) \times 10^{41}$ erg s^{-1}. From case F1 in Table 1 (e.g. each source experiences a different intrinsic absorption) one obtains ECFs of 4.225×10^{-2} for the N and 6.0×10^{-2} for the E sources. The corresponding intrinsic fluxes and luminosities are then $f^{\rm N} = (11.5 \pm 1.1) \times 10^{-13}$ and $f^{\rm E} = (4.13 \pm 0.6) \times 10^{-13}$ erg s^{-1} cm^{-2} e.g. $(2.2 \pm 0.2) \times 10^{41}$ and $(7.9 \pm 1.1) \times 10^{40}$ erg s^{-1} for N and E, respectively. The summed luminosity of $\sim 3 \times 10^{41}$ erg s^{-1} is again compatible to the $L_{\rm X} \sim 2.7 \times 10^{41}$ erg s^{-1} obtained from the fit. In summary, both estimates yield consistently for component E an X-ray luminosity of $\sim 8 \times 10^{40}$ erg s^{-1} and a luminosity ranging between 1.5 and 2.2 $\times 10^{41}$ erg s^{-1} for the nuclear source.

3.3. Extent of the components

The assessment of the true extent of compact sources revealed by the HRI may be complicated by the fact that, in an individual pointing, the theoretical resolution of the ROSAT HRI camera ($\sim 5''$) may be degraded by residual errors in the correction for the periodic wobbling of the satellite. Such errors may cause elongations in point sources on scales of $\lesssim 10''$ (cf. David et al. 1993) and lead to inflated radial intensity profiles.

Fig. 7 shows the background-subtracted intensity profiles of both X-ray components in NGC 7714 as derived from the smoothed ROSAT HRI map (Fig. 6). The total intensity profile of NGC 7714, containing some additional faint emission at levels below $\sim$ 10 counts ksec^{-1} arcmin^{-2} is shown by filled squares. The thick curve shows an empirical approximation to the on-flight PRF of the ROSAT HRI (David et al. 1993) convolved with the same smoothing function as the one applied

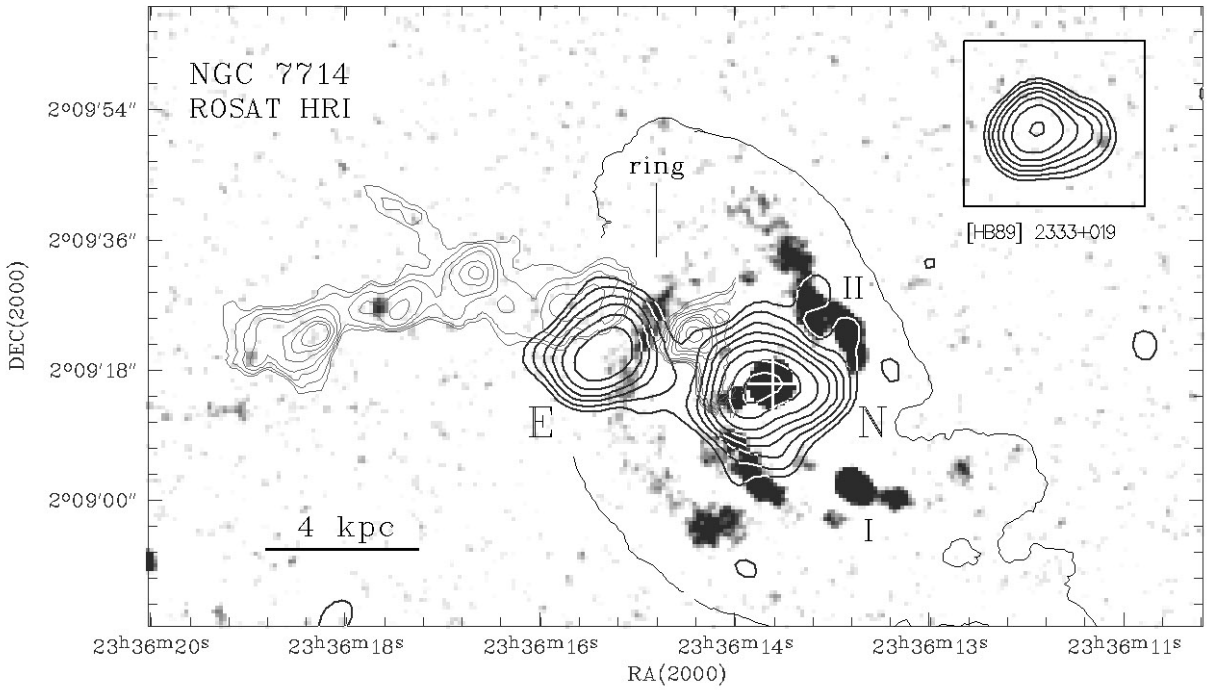

Fig. 6. Contour map of the X-ray emission of NGC 7714 (*thick lines*) as obtained from the ROSAT HRI image, overlaid to a R-band image. The ROSAT HRI map was smoothed with a Gaussian with fwhm=5″. The optical image was processed by the hb-method (Sect. 2) to better visualize fine features in the central region of NGC 7714. X–ray contours correspond to intensity levels of 8, 12, 18, 25, 35, 50, 75 and 100 $\mathrm{counts\ ksec^{-1}\ arcmin^{-2}}$ *above* the background (4.3±0.8 $\mathrm{counts\ ksec^{-1}\ arcmin^{-2}}$). The inset to the top-right shows the X–ray contours of the background QSO [HB89] 2333+019 at equal levels. The optical extent of NGC 7714 at the extinction-corrected surface brightness of 23 $\mathrm{R\ mag\ arcsec^{-2}}$ is shown by the outermost contour (*thin solid line*). Thin light contours delineate the VLA-detected H I-bridge eastwards of NGC 7714 (Smith et al. 1997). The X-ray emission of NGC 7714 is contributed by two distinct emitting regions with a count rate ratio ~ 2. The more luminous one (N) coincides with the nuclear starburst region while component E is located $\sim 20''$ eastwards of the nucleus, close to the outer boundary of the asymmetric stellar ring of NGC 7714 (Sect. 2). Contrary to the inactive region subtended by the stellar ring, the nuclear region (N) as well as features **I** and **II** are found to be strong Hα sources.

to the X–ray map (Fig. 6) and scaled to the maximum intensity of component E. Numerical integration of the smoothed PRF yields for its effective radius $r_{50} = 3\farcs3$ and for the radius containing 80% of the flux $r_{80} = 5\farcs9$. The corresponding quantities for each X-ray component, as obtained from profile integration to a threshold of 1 count ksec^{-1} arcmin^{-2}, are $r_{50} = (6\farcs4 \pm 0\farcs2)$ and $r_{80} = (10\farcs9 \pm 0\farcs25)$ for the nuclear component N and $r_{50} = (5\farcs6 \pm 0\farcs2)$ and $r_{80} = (9\farcs0 \pm 0\farcs3)$ for component E, thereby incompatible to those expected for a point source.

This result requires, however, a further check since, as pointed out above, the actual PRF of an individual HRI-pointing may differ from the nominal one.

For this purpose we assumed that the true PRF at the location of NGC 7714 can be approximated by the intensity distribution of the background QSO [HB89] 2333+019 (Fig. 7, thin line), located $\approx 3'$ off-axis the ROSAT HRI field. For the latter source we obtain $r_{50} = 4\farcs8$ and $r_{80} = 7\farcs7$, e.g. values by $\sim 40\%$ greater than those corresponding to the nominal PRF. The magnified PRF is presumably attributable to residual errors in the satellite's aspect solution rather than to the slightly degraded PRF at the off-axis angle of [HB89] 2333+019.

Nevertheless, the latter comparison demonstrates that the characteristic radii r_{50} and r_{80} for either X-ray emitting region in NGC 7714 are larger than both, the nominal and actual PRF of the ROSAT HRI exposure. Furthermore, it is relevant to the question of the extent of these components that, for intensities fainter than 30 counts ksec^{-1} arcmin^{-2}, their intensity distribution is systematically flatter than the one of the QSO. As a result, we conclude that the emission pattern of either X-ray emitting component in NGC 7714 is definitely incompatible with that of a point source.

4. Discussion

As mentioned in Sect. 3.2, attempts to disentangle the spectral nature of either extended X-ray source in NGC 7714 remained inconclusive due to the low angular separation of the knots and the relatively low number of received counts. Keeping in mind the uncertainties discussed in Sects. 3.1&3.2 we shall assume that both knots are emitting thermal bremsstrahlung with a mean plasma temperature ~ 0.5 keV ($\sim 6 \times 10^6$ K). Then the X-ray luminosity of component E is $L_{\rm X}^{\rm E}\ (0.1 - 2.4\,{\rm keV}) \sim 8 \times 10^{40}$ erg s^{-1}, while for the nuclear source we shall adopt the upper estimate of $L_{\rm X}^{\rm N}\ (0.1 - 2.4\,{\rm keV}) \sim 2 \times 10^{41}$ erg s^{-1} (cf.

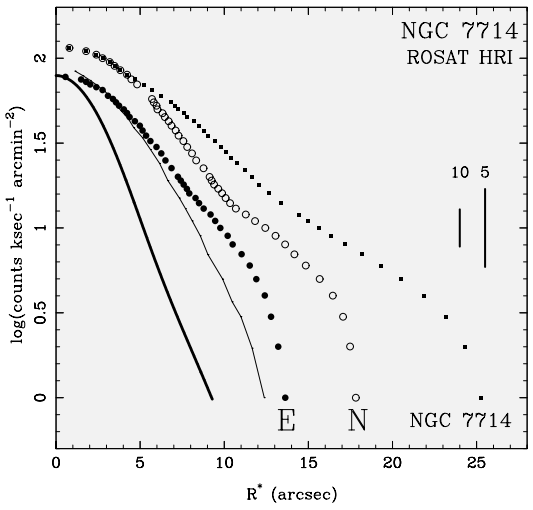

Fig. 7. Background subtracted intensity profiles of either X-ray emitting region revealed in NGC 7714 by the ROSAT HRI (Fig. 6). Both profiles were derived from the HRI-exposure after it was convolved with a Gaussian with fwhm=5″. The intensity profiles of the eastern (E) and the nuclear (N) component in units of $\mathrm{counts\ ksec^{-1}\ arcmin^{-2}}$ are shown with open and filled circles, respectively. The total emission at NGC 7714 is displayed by filled squares. The empirical approximation to the on-flight PRF of ROSAT HRI, convolved with a Gaussian with fwhm=5″ and scaled to the maximum intensity of component E, is shown by the thick curve. The thin solid line shows the intensity profile of the background QSO [HB89] 2333+019 located 3′ off-axis. The bars to the right indicate typical 2σ uncertainties at levels of 5 and 10 $\mathrm{counts\ ksec^{-1}\ arcmin^{-2}}$.

Table 2. Properties of the X-ray components

Component	N	E
Net counts	221±22	112±16
Count Rate (counts ksec^{-1})	4.85±0.46	2.48±0.36
Softness Ratio$^{\alpha}$	1.1±0.2	1.6±0.5
r_{50}^{β}	6.″4±0.″2	5.″6±0.″2
r_{80}^{c}	10.″9±0.″25	9.″0±0.″3
f_{X}^{d}	∼11.5	~ 4
L_{X}^{e}	∼2	~ 0.8

α: HRI *softness ratio* determined as the ratio of the net counts received in the HRI channels 1–5 and 6–11 (cf. Wilson et al. 1992).
β,c: Radii enclosing 50% and 80% of the flux, as determined from the intensity profiles (Fig. 7).
d;e: Intrinsic flux and luminosity in the ROSAT energy band (0.1–2.4 keV) in units of $10^{-13}\ \mathrm{erg\,s^{-1}\,cm^{-2}}$ and $10^{41}\ \mathrm{erg\ s^{-1}}$, respectively. Both quantities are derived on the assumption that the X-ray emission in either component can be approximated by a *thbr* model and shares the same spectral properties.

Sect. 3.2). In Sects. 4.1&4.2 we shall investigate physical processes accounting for the morphological and energetic X-ray properties of each emitting component.

4.1. Nuclear energy source

From the surface brightness profile of NGC 7714 (Fig. 2) we estimate the extinction corrected magnitude of the starburst nucleus to 13.5 mag. At the adopted distance of 40 Mpc to NGC 7714 the latter value translates to an absolute magnitude of $M_{\mathrm{R}} \approx -19.5$ mag. According to Bernlöhr (1993) the photometric properties of the nuclear region in NGC 7714 can be accounted for by an ongoing burst of star formation of age $\tau_{\mathrm{burst}} \sim 20$ Myr. Scaling the model predictions of Leitherer & Heckman (1995, hereafter LH95) to the observed nuclear luminosity and assuming continuous star formation over τ_{burst}, we obtain an average star formation rate (SFR) of $\approx 2.2\,\mathrm{M_{\odot}\ yr^{-1}}$. Hereby, we adopt a Salpeter initial mass function ($\alpha = 2.35$), solar metallicity and lower and upper stellar mass cutoffs of $1\,\mathrm{M_{\odot}}$ and $100\,\mathrm{M_{\odot}}$, respectively. We shall remark that the above model-dependent quantities are approximative only and represent a lower limit for the actual SFR in NGC 7714 as being derived by other authors from detailed spectrophotometric studies. For instance, from the Hα -luminosity of NGC 7714 Storchi-Bergman et al. (1994) deduced a SFR of $17.2\,(75/\mathrm{H_0})^2$ $\mathrm{M_{\odot}\ yr^{-1}}$. Furthermore, Calzetti (1997) has inferred from UV-to-NIR synthesis studies a SFR of $2.8 \div 12.2\,(75/\mathrm{H_0})^2\,\mathrm{M_{\odot}\ yr^{-1}}$ and deduced a much lower starburst age of ~ 10 Myr.

Scaling Figs. 2&6 of LH95 to the adopted SFR we obtain for the present evolutionary age of the nuclear starburst a number $N_{\mathrm{O*}} \approx 7 \times 10^4$ of O stars and a SN rate $\dot{SN} \approx 0.022\,\mathrm{yr^{-1}}$. The corresponding production rate of *mechanical* energy injected into the ISM by massive stars and SNe is $\dot{E}_{\mathrm{m}} \approx 8.8 \times 10^{41}$ $\mathrm{erg\ s^{-1}}$(LH95, Fig. 56) and the total *mechanical* energy generated since the onset of the starburst is $E_{\mathrm{m}} \approx 4.4 \times 10^{56}$ erg (LH95, Fig. 58).
The X-ray luminosity from O stars is $\sim N_{\mathrm{O*}} \cdot 10^{33}\ \mathrm{erg\ s^{-1}}$ $\simeq 7 \times 10^{37}\ \mathrm{erg\ s^{-1}}$. Given an average X-ray luminosity of $L_{\mathrm{X}}^{\mathrm{SNR}} \approx 2 \times 10^{36}\ \mathrm{erg\ s^{-1}}$ over a time scale $\tau_{\mathrm{SNR}} \sim 2 \times 10^4$ yr for a SN remnant (Cowie et al. 1981, Williams et al. 1997) we estimate the contribution of such sources to $\tau_{\mathrm{SNR}} \cdot \dot{SN} \cdot L_{\mathrm{X}}^{\mathrm{SNR}} \approx$ $9 \times 10^{38}\ \mathrm{erg\ s^{-1}}$ or $< 1\%$ of $L_{\mathrm{X}}^{\mathrm{N}}$. From the number ratio of $c_1 \sim 2 \times 10^{-3} \ldots 10^{-3}$ of O-stars to High Mass X-ray Binaries (HMXBs; Fabbiano et al. 1982) we obtain an upper limit of 140 currently active HMXBs in the nuclear starburst region of NGC 7714. With a typical X-ray luminosity of a HMXB of $\sim 10^{38}$ $\mathrm{erg\ s^{-1}}$ this results in a maximum luminosity contribution of this type of objects of the order of $1.4 \times 10^{40}\ \mathrm{erg\ s^{-1}}$. In summary, the direct contribution of X-ray emitting point sources produced by the nuclear starburst, such as O stars, SNRs and HMXBs amounts to $\sim 1.5 \times 10^{40}\ \mathrm{erg\ s^{-1}}$ or $\lesssim 10\%$ of $L_{\mathrm{X}}^{\mathrm{N}}$. This percentage will not be greatly enhanced even when postulating the presence of a few *super-Eddington* point-like sources with luminosities of $1.4 - 5 \times 10^{39}\ \mathrm{erg\ s^{-1}}$ as found in some nearby starburst galaxies (Dahlem et al. 1994, Vogler & Pietsch 1997, Wang et al. 1995, Fabbiano et al. 1997).

As a result, $\sim 90\%$ of the X-ray luminosity confined to the starburst nucleus of NGC 7714 must be attributed to the emission by extended hot gas (few $\times 10^6$ K) being heated up by the injection of *mechanical* energy from OB stars and SNe.

Eq. 3.2 of Nulsen et al. (1984) yields for the required mass of the hot plasma in the nuclear region of NGC 7714

$$\frac{M^{\rm N}_{\rm hot}}{\rm M_\odot} \approx$$

$$1.73\times10^5 \left(\frac{r}{100\rm pc}\right)^{\frac{3}{2}} \left(\frac{L^{\rm N}_{\rm X}}{10^{40}}\right)^{\frac{1}{2}} \left(\frac{\Lambda(T)}{5\times10^{-23}}\right)^{-\frac{1}{2}} \eta^{\frac{1}{2}} \qquad (1)$$

where r is the radius of the volume in pc, $\Lambda(T)$ the emission measure in 10^{-23} erg s^{-1} cm^3, and η the volume filling factor. Assuming for the emitting volume of component N a radius of 1 kpc and a mean plasma temperature $\sim 6\times10^6$ K we obtain a nominal gas mass $M^{\rm N}_{\rm hot} < 3\times10^7\times\sqrt{\eta}\,{\rm M_\odot}$. Thus, the mass of the hot plasma required to explain the nuclear X-ray luminosity of NGC 7714 is comparable to the stellar mass formed in the burst. The radiative output of the hot gas ($\sim 2\times10^{41}$ erg s^{-1}) corresponds to roughly 20% of the current *mechanical* energy output provided by the nuclear stellar population. Thus, there is no fundamental energy problem for the starburst hypothesis.

4.2. Eastern X-ray component

The absence of signatures of recent star formation at the stellar ring close to component E (Sect. 1) excludes the possibility that its X-ray luminosity of $\sim 8\times10^{40}$ erg s^{-1} is due to a superposition of point sources such as HMXBs and SNRs. Next we shall investigate whether the extended emission observed in region E is not intrinsic to NGC 7714 but due to the superposition of at least two foreground or background sources. As pointed out in Sect. 2, the estimated detection limit of the CCD-frame (Fig. 1) is ~ 20.3 R mag. This limit can effectively be pushed down by $\gtrsim 1$ mag when applying the hb-method. At this level, ground-based images do not reveal any optical point sources coincident with component E. The only conspicuous feature seen in an archival HST-WFPC2 exposure of NGC 7714 at a distance $\delta_{x,y}$=+16.″7, +5.″1 from the nucleus is a pair of two faint point sources being separated by $\approx 0.''2$. Their apparent R magnitude, estimated to 22.8 mag, is equivalent to that of a M5V star ($M_{\rm R}=+10.5$; Johnson 1966) at a distance of $\sim$ 2.9 kpc. The X-ray luminosity of such late-type stellar sources amounts to $5\div15\times10^{27}$ erg s^{-1} (Schmitt & Snowden 1990, Hünsch & Schröder 1996). At the assumed distance of 2.9 kpc, a source of this type would produce an X-ray flux $\sim 10^{-17}$ erg s^{-1} cm^{-2}, much lower than the detection threshold of ROSAT. Analogously we can excluse other candidates of foreground and background sources as origins for component E. We have made detailed checks on the possibilities of the contamination by Pop II binaries, background clusters and diffuse background sources (Hasinger et al. 1993).

We, therefore, conclude that the extended X-ray flux detected at the location of component E be a superposition of point sources of known type to be extremely improbable. Given that a physical intersection between the eastern H I-bridge (Smith et al. 1997) and NGC 7714 is likely, we consider below (*i*) a starburst wind interaction with the low-density halo or with the dense H I-bridge and (*ii*) collisions of H I clouds resulting from gas infall from the bridge including the interaction of the rotationally moving disk clouds with the material of the bridge.

4.2.1. Starburst-driven outflow

Theoretical and observational work in the past decade has advanced a picture where gas heated up by the central energy source is able to penetrate the ambient H I-layer and then to escape into the galactic halo with velocities of the order of 10^3 km s^{-1} (Chevalier & Clegg 1985, Heckman et al. 1987, Norman & Ikeuchi 1989 and references therein) where it produces an extended shock region. This mechanism could cause component E. The presence of wind of warm gas with a velocity $\sim$ 150 km s^{-1} with its axis pointing to the NE of the nuclear region is already suggested by optical spectroscopy (Taniguchi et al. 1988). Although the spectra do not prove a large-scale outflow of hot gas towards the galactic halo they show, however, the gas phase in NGC 7714 to be kinematically perturbed.

Suchkov et al. (1994, hereafter SBHL94) have shown that in a nuclear starburst-wind the bulk of the soft (0.2–2.2 keV) X-ray photons will not be produced in the wind material itself but rather by its collisionally shocked interface with the ambient halo gas. By analogy to the model prediction of SBHL94, component E could be interpreted as the shell of a hot cavity expanding from the nuclear starburst, with the wind material itself being too hot ($\sim 10^8$ K) to make a measurable flux contribution to the ROSAT energy band. Read & Ponman (1998) have presented a thorough discussion on unipolar outflows of hot gas seeming not to be unusual among colliding galaxies in a mid-stage of merging. An unipolar structure seems to readily evolve when injection occurs above the galaxy plane (Mac Low & McCray 1988) or in the presence of a kinematically disturbed ISM.

Models A1 and A2 of SBHL94 are computed assuming starburst properties similar to those we have adopted for NGC 7714, e.g. a SFR of 2 M$_\odot$yr^{-1}, Salpeter IMF and $\tau_{\rm burst}=17$ Myr and yield a number of predictions in accord with the present observations. For instance the luminosity of component E can be accommodated by a wind-halo interaction model when assuming a halo density <5 cm^{-3}. However, in this model it is expected that the source will appear much more extended than the rather compact component E.

Alternatively, component E may be the result of the collision of a starburst-driven wind with the western boundary of the H I-bridge discovered by Smith et al. (1997). This would lead to the formation of a shocked interface at the radius where the ram pressure ($\rho_{\rm wind}\,u^2_{\rm wind}$) of the wind becomes equal to the ambient pressure of the H I-gas. As discussed in Tenorio-Tagle & Muñoz-Tuñón (1997), while the outer shock is going on sweeping up the ambient cold gas, the inner (reverse) shock will thermalize the wind to temperatures of $1.26\times10^8\,u_3^2$ K where u_3 is the wind velocity in units of 3×10^3 km s^{-1} . In this model, the adopted plasma temperature $\sim 6\times10^6$ K corresponds to a post-shock temperature generated by a velocity of the order of 700 km s^{-1}. Pressumably, such a process is going to produce

a relatively compact shocked interface with size comparable to the diameter of the western tip of the H I-bridge, yielding a better correspondence to the morphology of component E than the wind-halo interaction hypothesis.

In summary, the morphological and energetic properties of component E may be understood in terms of the collision of a starburst-driven wind with the eastern H I-bridge rather than collision with the tenuous halo-gas.

4.2.2. Cloud-cloud collisions in the cold gas

A further hypothesis for the origin of the X-ray emission in region E invokes gas infall from the eastern H I-bridge on the H I-disk of NGC 7714. As shown by Tenorio-Tagle (1982) the energy-release caused by an H I-cloud impinging on the disk can provoke a supersonic expansion of a hot (10^6–10^7 K) ring-shaped cavity in the ambient cold medium. Smith et al. (1997) were not able to confirm a systematic motion of the massive (1.5×10^9 $\mathrm{M}_\odot$) H I-bridge towards NGC 7714. Nevertheless, they measured a projected velocity dispersion > 100 km s^{-1} within the H I-bridge. Therefore, if the H I-bridge is intersecting the disk of NGC 7714 high-speed gas cloud collisions are likely to occur in the interaction zone.

If the infalling gas medium is composed of clouds with a radius $r_\mathrm{c} \sim 5$ pc and a volume filling factor $\eta = 0.1$ then the mean free path $(2/3)\,(r_\mathrm{c}/\eta)$ of an interloping cloud amounts to ~ 30 pc, thus less than the disk thickness of NGC 7714. Given the low sound speed in such a cloud (~ 0.7 km s^{-1} ; Spitzer 1978), a collision at a relative velocity $v_\mathrm{rel} \sim$ few 100 km s^{-1} would be characterized by a high Mach number, thus, give rise to a strong shock wave propagating within either cloud with a velocity $(4/3)(v_\mathrm{rel}/2)$ (Jog & Solomon 1992). From the latter considerations, a strip of shocked material with size comparable to r_{50} (~ 1 kpc) can be formed in a time span of few Myr when $v_\mathrm{rel} \sim 200$ km s^{-1} . Substituting the estimated intrinsic X-ray luminosity of component E and such a radius in Eq. (1) we obtain for the mass of the hot interior $M^\mathrm{E}_\mathrm{hot} \sim 1.5\times10^7 \times \sqrt{\eta}\,\mathrm{M}_\odot$. From Eq. (3) of Nulsen et al. (1984) the corresponding gas cooling time is $\tau_\mathrm{cool} \sim 15\,\sqrt{\eta}$ Myr. An estimate of $\sim 3.8\times10^{55}\times\sqrt{\eta}$ erg for the energy content of component E can be inferred assuming a constant radiation of $\dot{E} \equiv L^\mathrm{E}_\mathrm{X} \simeq 8 \times 10^{40}$erg s^{-1} over τ_cool. This is equivalent to the kinetic energy of a cloud with mass $\sim 6 \times 10^7$ $\mathrm{M}_\odot$ (~ 4% of the mass of the H I-bridge) plunging onto the disk of NGC 7714 with a velocity v_rel.
From the virial mass of 2×10^{10} $\mathrm{M}_\odot$ within a radius of 15″ inferred for NGC 7714 by Bernlöhr (1993) and assuming rotational motions one obtains at the distance of component E a circular velocity of ~ 150 km s^{-1}. Thus, the required collisional velocity v_rel is already comparable to the average circular gas velocity in the disk of NGC 7714.
As a result, the release of kinetic energy at region E can be understood in a twofold manner: gas infall onto the disk by analogy to Galactic *worms* (Heiles 1979, Mirabel 1982) and/or collision of rotationally moving H I-clouds of the disk of NGC 7714 with the western boundary of the H I-bridge. Clearly, a number of parameters must be specified to assess the energy output of these processes. Most important, the H I-kinematics and the thermalization efficiency during such a collision remains uncertain. Nevertheless, we argue that in view of the energetics such a mechanism powered by cloud collisions only can readily account for the observed X-ray luminosity in component E.

4.2.3. On the fate of component E

Reinfall of tidally ejected matter is likely to be a frequent occurrence in the merging of two gas-rich galaxies (Hibbard & Mihos 1995) and may well be accompanied by processes discussed in Sects. 4.2.1&4.2.2 generating X-ray emission. However, it is difficult to analyze how such processes depend on the kinematical, dynamical and geometrical circumstances of the merging event. While Read & Ponman (1998) do not report the presence of any strong extranuclear features they find the clear presence of low-surface-brightness extended X-ray emission in their sample. They discuss the possibility that such X-ray halos seen in evolved mergers do not form entirely through the starburst-driven ejection of hot gas from the nucleus, but also through infalling shock-heated tidal matter.

If component E is due to a systematic gas infall from the bridge one may speculate about the observability of this feature. Among the fifteen thoroughly investigated colliding systems shown in Fig. 5 only Arp 284 exhibits a high-surface-brightness extranuclear X-ray component. Assuming that the formation of such features in the interaction region must commonly occur at some stage during the collision lasting $\sim 10^9$ yr, then from a statistical point of view this feature cannot survive much longer than 10^8 yr.

This time-scale does not seem unreasonable: as discussed above, the initial impact between two cold media with a velocity of a few $\times$ 100 km s^{-1} can readily give rise to the formation of a shocked interface. Subsequent infall of cold gas occurring with a velocity smaller than the internal sound speed in the hot cavity is not expected to add much to the shock-induced luminosity. The period of visibility of such a shock-region (identified with region E of Arp 284) will be of the order of its cooling time $\tau_\mathrm{cool} \lesssim 10^8$ yr. While mass-loading of the hot cavity enhances the cooling efficiency, differential rotation may smear the high-surface-brightness X-ray features (again on a time-scale $\sim 10^8$ yr), thus contributing to the formation of a diffuse low-surface-brightness X-ray halo similar to those found by Fricke & Papaderos (1996) and Read & Ponman (1998).

5. Summary and conclusions

Numerical simulations suggest that Arp 284 is the result of an off-center encounter between the spiral galaxies NGC 7714/15 (Smith et al. 1997). The less massive one, NGC 7715, underwent a burst of star formation ~ 70 Myr ago, presumably at the time of the closest passage between both systems. While NGC 7715 is at present in a quiescent post-starburst phase, its interacting neighbour NGC 7714 (Smith et al. 1997) being by a factor ~ 3 more massive harbours an ongoing nuclear starburst initiated $\lesssim 20$ Myr ago (Bernlöhr 1993, Calzetti 1997).

Morphological signatures of the interaction in Arp 284 are a conspicuous stellar ring in NGC 7714 to the east of its nucleus and a faint ($\mu_{\rm R} \gtrsim 23$ mag arcsec^{-2}) stellar bridge probably connecting NGC 7715 and NGC 7714. Smith et al. (1997) have discovered a massive ($\sim 1.5\times10^9\,{\rm M}_\odot$) H I-bridge parallel to the stellar one, likely being of tidal origin. Both features intersect NGC 7714 roughly 20″ eastwards of its nuclear region, near to the outer boundary of the stellar ring.

The surface brightness distribution of NGC 7714 shows two distinct luminosity parts in excess of its disk brightness. On small scales ($R^* \lesssim 5''$) the light is being dominated by its compact high surface brightness ($\mu_{\rm R} < 16$ mag arcsec^{-2}) starburst nucleus. At intermediate intensity levels and out to a radial extent equivalent to two disk scale lengths the intensity distribution of NGC 7714 shows an initially flat and then sharply decreasing plateau. This feature is partly due to the luminosity of the stellar ring mentioned above.

In agreement to results from *Einstein*, ROSAT PSPC observations show that the entire emission in Arp 284 is confined to NGC 7714. Fits to the ROSAT PSPC spectrum imply a thermal emission origin approximated best by a thermal bremsstrahlung model with kT$\sim$0.4$\div$0.6 keV ($4.6 \div 7 \times 10^6$ K). We deduce an intrinsic 0.1–2.4 keV luminosity of NGC 7714 ranging between 2 and $\sim 4.4\times10^{41}$ erg s^{-1}, comparable to the luminosity reported for other interacting/merging starburst systems.

ROSAT HRI maps reveal that the soft X-ray luminosity of NGC 7714 is being contributed by two distinct X-ray emitting sources both of which were found to be extended. The more luminous one (N), for which we estimate an X-ray luminosity $\lesssim 2\times10^{41}$ erg s^{-1} is coincident with the starburst nucleus of NGC 7714. Its luminosity can be accounted for by the superposition of point- and diffuse X–ray emitting sources expected to form in a starburst. Point sources evolving in a continuous nuclear starburst with an age ~ 20 Myr and average SFR $\sim 2\,{\rm M}_\odot$ yr^{-1} are estimated to provide only a minor fraction (~ 10%) of the nuclear X–ray luminosity in NGC 7714 while the bulk of the soft X-ray emission is being produced by hot ISM residing in a volume $\lesssim 2$ kpc in diameter.

The second X–ray source (component E), located roughly 20″ eastwards of the starburst nucleus is of intriguing nature. It lacks any optical counterpart and the probability for confusion with an assembly of X-ray point sources unrelated to Arp 284 is low. We estimate the intrinsic X-ray luminosity of this component to $\sim 8 \times 10^{40}$ erg s^{-1} and favour a model based on *in situ* shock–heated gas. With respect to the combined evidence of VLA- and ROSAT HRI maps different interpretations seem possible. One plausible scenario invokes the collision of a starburst–driven wind with the western boundary of the massive H I-bridge. In this case a relatively compact shocked layer with a temperature of few 10^6 K may evolve. Alternatively, gas–infall from the eastern H I-bridge onto the disk of NGC 7714 with a speed comparable to the intrinsic disk velocity dispersion can produce a collisional interface powering component E. Collisional breaking of the disk-rotation in NGC 7714 by H I-clouds contributes an additional energy source. We argue that the X-ray spot is a transient phenomenon and may eventually evolve into an extended low-surface-brightness X-ray halo as commonly observed in merging systems.

Acknowledgements. This work was supported by the Deutsche Agentur für Raumfahrtangelegenheiten (DARA) grant 50 OR 9407 6. We wish to thank an anonymous referee for useful comments which have helped to clarify various aspects of this work. This research has made use of the NASA/IPAC extragalactic database (NED) which is operated by the Jet Propulsion Laboratory, Caltech, under contract with the National Aeronautics and Space Administration.

References

Arp, H.C. 1966, Atlas of Peculiar Galaxies (Pasadena: Caltech)
Barnes, J.E., Hernquist, L. 1992, ARA&S 30, 705
Barnes, J.E., Hernquist, L. 1996, ApJ 471, 115
Bernlöhr, K., 1993, A&A 268, 25
Bischoff, K., Kollatschny, W., Pietsch, W. 1996, in *Röntgenstrahlung from the Universe*, eds. H.U. Zimmermann, J.E. Trümper, H. Yorke, 423
Bushouse, H.A., Werner, M.W. 1990, ApJ 359, 72
Calzetti, D. 1997, AJ 113, 162
Chevalier, R.A., Clegg, A.W. 1985, Nature 317, 44
Cowie, L.L., McKee, C.F., Ostriker, J.P. 1981, ApJ 247, 908
Dahlem, M., Hartner, G.D., Junkes, D. 1994, ApJ 432, 598
David, L.P., Jones, C., Forman, W. 1992, ApJ 388, 82
David, L.P., Harnden, F.R.,Jr., Kearns, K.E., Zombeck, M.V. 1993, The ROSAT High Resolution Imager (HRI) (Technical Rep., US ROSAT Science Data Center/SAO)
Devereux, N.A., Eales, S.A. 1989, ApJ 340, 708
Dickey, J.M. & Lockman, F.J. 1990, ARA&A 28, 215
Duc, P.-A., Mirabel, I.F. 1994 A&A 289, 83
Fabbiano, G., Feigelson, E., Zamorani, G. 1982, ApJ 256, 397
Fabbiano, G., Kim, D.-W., Trinchieri, G. 1992, ApJS 80, 531
Fabbiano, G., Schweizer, F., Mackie, G. 1997, ApJ 478, 542
Fricke, K.J., Kollatschny, W. 1989, Proc. of IAU Symp. No. 134, 425
Fricke, K.J., Papaderos, P. 1996, in *Röntgenstrahlung from the Universe*, eds. H.U. Zimmermann, J.E. Trümper, H. Yorke, 377
González-Delgado, R.M., Pérez, E., Díaz, Á.I., García-Vargas, M.L., Terlevich, E., Vilchez, J.M. 1995, ApJ 439, 604
Güdel, M., Kürster, M. 1996, in *Röntgenstrahlung from the Universe*, eds. H.U. Zimmermann, J.E. Trümper, H. Yorke, 37
Hasinger, G., Trümper, J., Schmidt, M. 1991, A&A 246, L2
Hasinger, G., Burg., R., Giacconi, R., Hartner, G., Schmidt, M., Trümper, J., Zamorani, G. 1993, A&A 275, 1
Heckman, T.M., Armus, L., Miley, G.K. 1987, AJ 93, 276
Heckman, T.M., Dahlem, M, Eales, S.A., Fabbiano, G., Weaver, K. 1996 ApJ 457, 616
Heiles, C.E. 1979, IAU Symp. 184, ed. W.B. Burton, 301
Hernquist, L. 1992, ApJ 400, 460
Hewitt, A., Burbidge, G. 1989, ApJS 69, 1
Hibbard, J.E., Mihos, J.C. 1995, AJ 110, 140
Hibbard, J.E., van Gorkom, J.H. 1996, AJ 111, 655
Higdon, J.L. 1988, ApJ 326, 146
Hünsch, M., Schröder, K.-P. 1996, A&A 309, L51
Jog., C.J., Solomon, P.M. 1992, ApJ 387, 152
Johnson 1966, AR&AA 4, 193
Kollatschny, W., Kowatsch, P., Fricke, K.J. 1996, in *Röntgenstrahlung from the Universe*, eds. H.U. Zimmermann, J.E. Trümper, H. Yorke, 383
Leitherer, K., Heckman, T.M. 1995, ApJS 96, 9

Lynds, R., Toomre, A., 1976, ApJ 209, L382
Mac Low, M.-M., McCray, R. 1988, ApJ 324, 776
Mihos, J.C., Hernquist, L. 1996, ApJ 464, 641
Mirabel, I.F. 1982, ApJ 256, 112
Morse, J.A. 1994, PASP 106, 675
Norman, C., Ikeuchi, S. 1989, ApJ 345, 372
Norman, C.A., Bowen, D.V., Heckman, T., Blades, C., Danly, L. 1996, ApJ 472, 73
Nulsen, P.E.J., Steward, G.C., Fabian, A.C. 1984, MNRAS 208, 185
Papaderos, P. & Fricke, K.J. 1998, in preparation
Pfefermann E., Briel U.G., Hippmann H., et al., 1987, Proc. SPIE 733, 519
Raymond, J.C., Smith, B.W. 1977, ApJS 35, 419
Read A.M., Ponman T.J., Wolstencroft R.D. 1995, MNRAS 277, 397
Read A.M., Ponman T.J., Strickland, D.K. 1997, MNRAS 286, 626
Read, A.M., Ponman, T.J. 1998, MNRAS 297, 143
Sanders, D.B., Mirabel, I.F. 1996, ARA&A 34, 749
Schmitt, J.H.M.M., Snowden, S.L. 1990, ApJ 361, 207
Schweizer, F. 1982, ApJ 252, 455
Smith, B.J. 1991, ApJ 378, 39
Smith, B.J., Wallin, J.F. 1992, ApJ 393, 544
Smith, B.J., Struck, C., Pogge, R.W. 1997, ApJ 483, 754
Solomon, P.M., Downes, D., Radford, S.J.E. 1992, ApJ 387, L55
Spitzer, L. 1978, Physical Processes in the Interstellar Medium (New York: John Wiley)
Storchi-Bergmann, T., Calzetti, D., Kinney, A.L. 1994, ApJ 429, 572
Suchkov, A.A., Balsara, D.S., Heckman, T.M., Leitherer, C. 1994, ApJ 430, 511
Sulentic, J.W. 1990, IAU Colloquium 124, 291
Taniguchi, Y., Kawara, K., Nishida, M., Tamura, S., Nishida, M.T. 1988, AJ 95, 1378
Telles, E., Terlevich, R. 1997 MNRAS 286, 183
Tenorio-Tagle, G. 1982, A&A 88, 61
Tenorio-Tagle, G., Muñoz-Tuñón, C. 1997, ApJ 478, 134
Toomre, A., Toomre, J. 1972, ApJ 178, 623
Trümper J., 1983, Adv. Space Res. 2, 241
Tully, R.B. 1988, Neraby Galaxies Catalog, Cambridge University Press, Cambridge
Veilleux, S., Cecil, G., Bland-Hawthorn, J., Tully, R.B., Filippenko, A.V., Sargent, W.L.W. 1994, ApJ 433, 48
Voges, W., Gruber, R., Paul, J. et al. 1992, in *Proc. European ISY conference*, eds. T.D. Guyenne, J.J. Hunt, 223
Vogler, A., Pietsch, W. 1997, A&A 319, 459
Wang, Q.D., Walterbos, R.A.M., Steakley, M.F., Norman, C.A., Braun, R. 1995, ApJ 439, 176
Wang J., Heckman, T.M., Weaver, K.A., Armus, L., 1997 ApJ 474, 659
Weedman, D., Feldman, F.R., Balzano, V.A., Ramsey, L.W., Sramek, R.A., Wu, C.-C. 1981, ApJ 248, 105
Williams, R.M., Chu, Y.-H., Dickel, J.R., Beyer, R., Petre, R., Smith, R.C., Milne, D.K. 1997, ApJ 480, 618
Wilson, A.S., Elvis, M., Lawrence, A., Bland-Hawthorn, J. 1992, ApJ 391, L75
Zimmermann, H.-U. et al. 1994, EXSAS User Guide, 4th edition